

The SuperCDMS experiment: Status and prospects

E. MICHIELIN(*)

University of British Columbia and TRIUMF - Vancouver, Canada

received 19 September 2022

Summary. — The Super Cryogenic Dark Matter Search (SuperCDMS) experiment is one of the leading role actors in the search for Dark Matter (DM), focusing on particles with masses below $10 \text{ GeV}/c^2$. After its successful campaign in the Soudan Underground Laboratory, the project is preparing for its next phase moving to the SNOLAB laboratory in Sudbury, Canada. Improved detector technologies and the new experiment set-up will allow to push the sensitivity to lower masses, down to about $0.5 \text{ GeV}/c^2$ for Weakly Interacting Massive Particles (WIMPs) and to improve the cross-section reach by more than one order of magnitude. One key ingredient for the experiment's success is the precise knowledge of the ionization yield in silicon (Si) and germanium (Ge) at low energy. This manuscript, after briefly describing the SuperCDMS status and prospects, reports the measurement of the ionization yield in Ge performed by the collaboration using data from the previous campaign in Soudan.

1. – Introduction

Although numerous evidences from Cosmology and Astrophysics [1] indicate the existence of Dark Matter (DM), all the experimental attempts to directly detect particles that may constitute dark matter have been unsuccessful. During the last two decades, most efforts were focused on the search for the so-called Weakly Interacting Massive Particles (WIMPs) [2] predicted by supersymmetric models, with favored masses in the $10 \text{ GeV}/c^2$ to $10 \text{ TeV}/c^2$ range, both at the Large Hadron Collider and at DM direct detection experiments. The lack of discovery opened up the field and pushed for the consideration of additional, well-motivated theoretical models that predict DM particles with lower masses, such as asymmetric dark matter [3] and dark sectors [4]. The Super Cryogenic Dark Matter Search (SuperCDMS) experiment is designed to search for dark matter signals in the low-mass range ($< 10 \text{ GeV}/c^2$) using germanium (Ge) and silicon (Si) cryogenic detectors. The project is currently in its installation phase for the upcoming campaign that will take place in the SNOLAB underground laboratory in Sudbury,

(*) On behalf of the SuperCDMS Collaboration.

Ontario, Canada. One key ingredient for its success is the capability to calibrate its nuclear recoil energy scale, which for its most sensitive detectors depends on the knowledge of the ionization yields in Ge and Si.

2. – The SuperCDMS detector technology

The way to achieve sensitivity to sub-GeV mass DM particles is to push the detector energy threshold as low as possible, given the exponentially falling energy spectrum of the expected DM signals. SuperCDMS SNOLAB employs germanium and silicon cylindrical crystals of 100 mm in diameter and 33.3 mm in thickness, kept at cryogenic temperature (tens of mK), as the target to detect the interaction of DM particles. In the interaction, the energy transferred by the incoming particle to the nuclei and/or the electrons of the crystal lattice produces phonons (vibrations) that propagate in the crystal, as well as electron-hole pairs (ionization). The phonons are detected by transition edge sensors deposited on both sides of the crystal [5], while the electron-hole pairs are drifted by an electric field to the surfaces of the crystal. Two detector types have been designed based on this technology, the Interleaved Z-sensitive Ionization and Phonon (iZIP) and the High Voltage (HV) detectors. While they have common physical dimensions and are fabricated from the same materials using the same techniques, they differ in the bias voltage applied to drift the charges and geometry.

In the iZIP detectors, both flat surfaces are equipped with six phonon sensor channels that are grounded, while a voltage bias of ~ 5 V is applied across the two interleaved ionization sensor channels. Being able to measure both the ionization and the phonon signals, these detectors can distinguish between electron recoil (ER) and nuclear recoil (NR) events by measuring the ionization yield, which is the energy ratio of ionization production to recoil energy. In ER events in fact, most energy goes into ionization compare to NR induced events. This effect allows efficient removal of all ER backgrounds and so exploration of new regions down in cross-section, but it is limited in threshold to ~ 1 keV and so to DM particle masses above ~ 5 GeV/ c^2 .

The HV detectors are designed for the best sensitivity at low energy. They are equipped with six phonon sensor channels on each face but without ionization sensors, allowing for a better phonon collection and therefore better phonon energy resolution. Of course, this means that these detectors cannot identify the type of interaction and so they are dominated by ER backgrounds. A larger bias voltage, up to 100 V, is applied. This is done in order to exploit the Luke-Trofimov-Neganov effect [6] [7] to boost the phonon signal in order to decrease the effective energy threshold of the detector. In fact, the electron-hole pairs generated in the interaction create phonons themselves while drifting in the crystal, with the additional phonon energy (E_{Luke}) proportional to their charges times the applied voltage bias. The total phonon energy (E_{Ph}), given the recoil energy E_R , can be calculated as:

$$(1) \quad E_{Ph} = E_R + E_{Luke} = E_R + \frac{y(E_R)E_R}{\epsilon} e\Delta V,$$

where $y(E_R)$ is the energy-dependent ionization yield, ϵ is the average energy required to create an electron-hole pair and $e\Delta V$ is the (positive) electron charge times the applied bias voltage. Eq. 1 shows that to reconstruct the E_R , the knowledge of the ionization yield for the energy range of interest is necessary. The HV detectors allow an energy

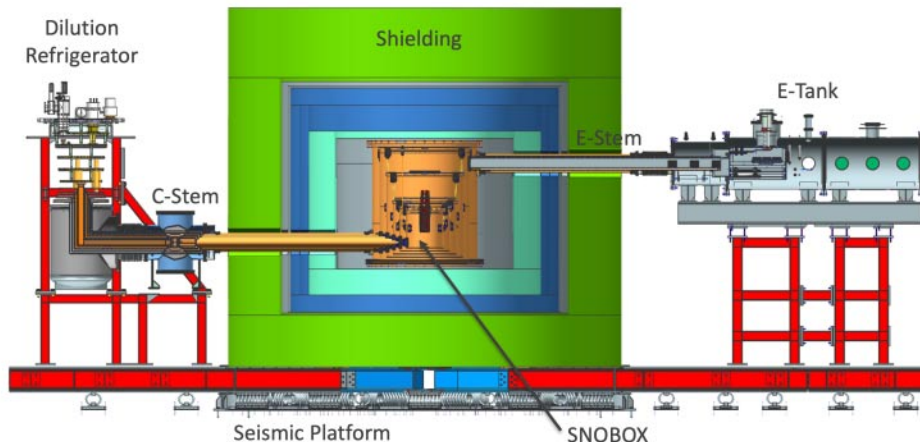


Fig. 1. – Schematic of the SuperCDMS SNOLAB experiment, highlighted are the dilution refrigerator, the copper cans that contain the detector towers, the tank for the warm electronics and the seismic isolation system.

threshold as low as ~ 100 eV and so detection of DM particle masses above ~ 0.5 GeV/ c^2 , but they will be limited in exposure due to the ER backgrounds.

3. – SuperCDMS at SNOLAB

The SuperCDMS detectors described in the previous section will be operated in the “ladder lab” drift in the SNOLAB underground laboratory, which is located approximately 2 km underground near Sudbury, Ontario, Canada. The rock overburden provides shielding against cosmic rays equivalent to 6010 meters of water, compared to the 2100 meter water equivalent of the previous site of the experiment at the Soudan Underground laboratory.

The initial payload will consist of 24 detectors, 10(2) Ge(Si) iZIPs and 8(4) Ge(Si) HVs, placed in 4 stacks (called ‘towers’) consisting of 6 crystals each. These towers will be cooled down to ~ 30 mK using a dilution refrigerator. The cold part of the full experiment is referred to as the SNOBOX, which consists of six cylindrical copper cans suspended by Kevlar ropes which provide shielding and thermal connection to the towers, with each can connected to a thermal stage of the refrigerator. The SNOBOX is surrounded by shielding to stop radiation from the cavern. A 40 cm thick polyethylene shield is used to absorb neutrons, followed by 23 cm of low-activity lead to shield from gamma radiation. The warm electronics of the experiment is mounted on a tank that is connected to the SNOBOX through what it is called E-stem. Detector control and readout cards (DCRC) have been developed with the capability of controlling the system and of reading out the detector signals. Finally, the whole system is mounted on a spring-loaded platform to isolate the experiment from any seismic activity. See [8] for more detailed information about the system. Figure 1 shows a sketch of the planned experiment.

TABLE I. – *The anticipated exposures and detector parameters for the SuperCDMS SNOLAB experiment, values taken from [10].*

	iZIP		HV	
	Ge	Si	Ge	Si
Number of detectors	10	2	8	4
Total exposure [kg·yr]	45	3.9	36	7.8
Phonon resolution [eV]	33	19	34	13
Ionization resolution [eV _{ee}]	160	180	–	–
Voltage Bias ($V_+ - V_-$) [V]	6	8	100	100

3.1. Status and prospects. – As of May 2022 the experiment is undergoing its installation phase. The radon filter system has been completely installed, as well as the seismic isolation platform. Successful trial assembly of the inner polyethylene and the outer lead shields occurred in an external facility, and now all the material is stored underground at SNOLAB. The dilution refrigerator has been constructed and is being tested at the Fermi National Accelerator Laboratory. The first Ge and Si HV prototypes are being operated underground at the Cryogenic Underground TEst (CUTE) [9] facility, which, being located at SNOLAB right beside SuperCDMS, it provides the perfect test bed for the study of their performance. The data acquisition system infrastructure has been installed, and the software has been fully tested during CUTE operations. All the detectors for the SuperCDMS SNOLAB payload have been fabricated, and the testing of the first iZIP tower is ongoing at the SLAC National Accelerator Laboratory. Everything is in place for the start of commissioning runs in 2023.

A detailed study of the projected sensitivity for nucleon-coupled DM interaction, with a thoughtful discussion of the expected backgrounds, can be found in ref. [8]. An updated calculation of the projected sensitivity has been recently published [10], which uses the latest known values for the detector resolutions and which accounts for ionization leakage in the HV detectors. The planned payload, detector performance, and anticipated total exposures for the SNOLAB experiment are shown in Tab.I which is taken from [10]. Using those values, the projected sensitivity for various DM models can be calculated. Figure 2 shows the sensitivity for DM particles interacting with nuclei, using both the optimum interval [11] (OI) and a profile likelihood-ratio method, with a comparison of the latest results with the older OI projections calculated in ref. [8].

Figure 3 instead, shows the sensitivity for DM particle scattering with electrons, calculated using the same assumptions presented in table I, using a profile-likelihood method. Only the HV detector is used for this projection, and three electron-coupled dark matter models are presented: dark photon, axion-like-particle, and dark-photon-coupled light dark matter.

These projections outline how SuperCDMS SNOLAB will be able to study and cover a large new parameter space for dark matter interactions both with nuclei and with electrons for masses below $5 \text{ GeV}/c^2$, complementing other experiments using other techniques in this range.

4. – The ionization yield

Eq. 1 describes how to calculate the recoil energy given the measured total phonon energy. As already discussed in sect. 2, the precision with which we can determine E_R

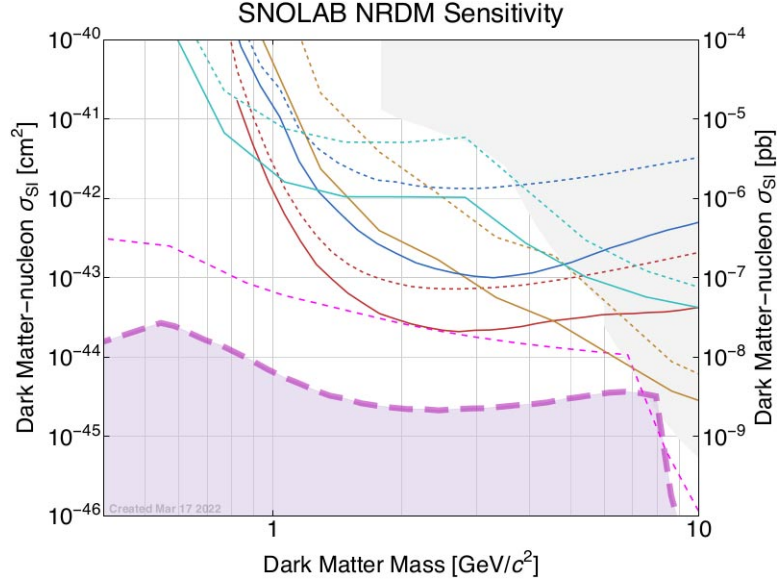


Fig. 2. – Optimum interval (dashed) and profile-likelihood ratio (solid) exclusion sensitivity at 90% CL for nucleon-coupled dark matter. Legend: (red-brown) Ge HV; (blue) Si HV; (mustard) Ge iZIP; (cyan) Si iZIP; (magenta long dashed and shaded) is the neutrino fog. Taken from [10].

in the HV detectors depends on the knowledge of the energy-dependent y parameter, the ionization yield, which is defined as the ratio of the ionization energy to the total recoil energy. Given the importance of a precise determination of the ionization yield at low energies, the SuperCDMS collaboration started a campaign to measure it in both Ge and Si. A paper describing a new measurement in Si is in preparation, meanwhile a new determination of y in Ge can be found in ref. [12], with a summary outlined in the following.

4.1. *The photo-neutron measurement.* – A semi-empirical parametrization for the ionization yield in semiconductors was established in 1963 by Lindhard [13], and while data from multiple experiments show a good agreement with this prediction for energies above ~ 10 keV, at lower energies the measurements disagree with the model; see for example ref. [14]. For a material with mass number A and atomic number Z , the Lindhard model predicts an ionization yield:

$$(2) \quad y(E_R) = k \frac{g(\epsilon)}{1 + kg(\epsilon)},$$

where:

$$(3) \quad g(\epsilon) = 3\epsilon^{0.15} + 0.7\epsilon^{0.6} + \epsilon; \quad \epsilon = 11.5 E_R Z^{-7/3}.$$

The parameter k is typically between 0.156 to 0.160 for stable isotopes of Ge.

At the end of its operations at Soudan, SuperCDMS took data with two gamma sources, ^{88}Y and ^{124}Sb , which were deployed sequentially and were placed on top of a ^9Be

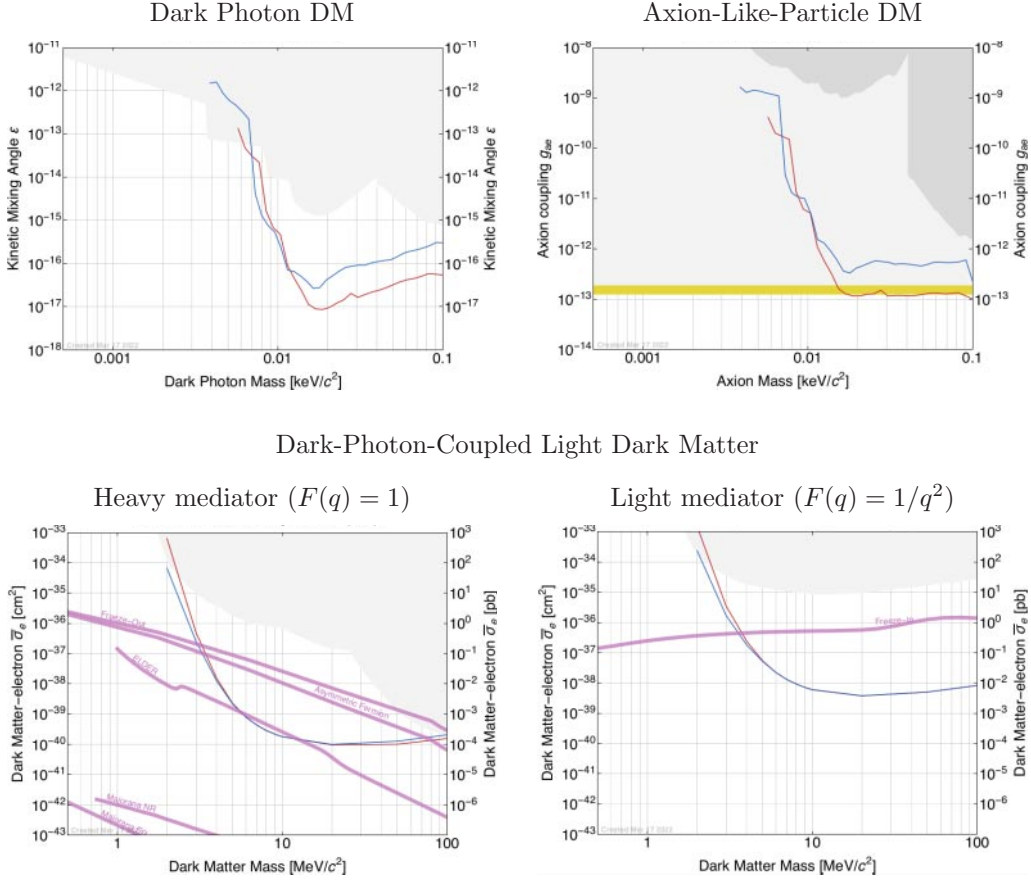


Fig. 3. – Projected sensitivity for electron-coupled dark matter, using the profile-likelihood ratio method at 90% CL for HV detectors (Si: blue; Ge: red). Light shaded regions show the outline of all current limits. (Top left) Dark photon sensitivity. (Top right) Axion-like-particle sensitivity. (Bottom) Dark-photon-coupled light dark matter sensitivity assuming a heavy mediator or a light mediator. Taken from [10].

disk. As a consequence of the photoproduction process, nearly mono-energetic neutrons were emitted from the ^9Be wafer, with an average energy of 152 keV for ^{88}Y and 24 keV for ^{124}Sb . Two Ge iZIP detectors (T5Z2 and T2Z1), run in HV mode biased at 70 V and 25 V respectively, were employed to measure the resulting neutrons. The photo-neutron data were taken for ~ 144 days between June 5th, 2015 and October 26th, 2015. Data were recorded both with the ^9Be wafer (neutron-ON) and without it (neutron-OFF).

The ionization yield is extracted from the data using a likelihood analysis which uses background and signal energy probability distribution functions (PDFs). The signal PDFs for the three data-taking configurations, ^{88}Y and ^{124}Sb with T5Z2, and ^{124}Sb with T2Z1, were generated using the simulation package Geant 4 [15]. The simulated energy recoil is converted to total phonon energy, and then smeared by the detector resolution model, using a modified Lindhard model, where the k value is allowed to vary linearly

TABLE II. – Summary of the k_{low} and k_{high} fit results along with their statistical and systematic uncertainties.

	Best fit value	Stat. uncertainty	Sys. uncertainty
k_{low}	0.040	0.005	0.008
k_{high}	0.142	0.011	0.026

with the energy:

$$(4) \quad k(E_r) = k_{\text{low}} + \frac{k_{\text{high}} - k_{\text{low}}}{E_{\text{high}} - E_{\text{low}}}(E_r - E_{\text{low}}),$$

with E_{low} and E_{high} the minimum and maximum nuclear recoil energy that the fit was sensitive to. We refer to k_{low} and k_{high} as the two components of a vector \vec{k} .

The background model is comprised of the dominant ER background component, which are the Compton-scattered photons from the sources off the electrons in the Ge crystal, and the K-, L- and M-shell electron capture x-rays. Both are described by analytic functions that are fitted to the neutron-OFF data to determine the Compton step sizes and the amplitude of the K-shell peak. The fit residuals, smoothed by applying a Gaussian filter, are finally added to the model to include any outstanding effect.

Given the signal and the background models, the negative log-likelihood function that is minimized to determine the best fit parameters is then defined as:

$$(5) \quad -\ln \mathcal{L} = - \sum_{D=1}^3 \sum_{i=1}^{N_D} \ln(f_D \nu_D(E_i, \vec{k}) + (1 - f_D)b_D(E_i)),$$

where N_D is the number of events in the data set D that pass a set of livetime, quality and threshold cuts, f_D is the fractional contribution of the neutron signal, $\nu_D(E, \vec{k})$ are the parameter-dependent signal PDFs, and $b_D(E)$ are the background PDFs. The free parameters are the three neutron contribution fractions f_D and the Lindhard parameters \vec{k} .

The systematic uncertainties due to the limited knowledge of the value of the Fano factors, due to the uncertainty on the background model shape, the uncertainty on the neutron elastic scattering cross section used to generate the signal model, and due to the choice of the specific neutron cross section library used, have been evaluated.

The best fit values of \vec{k} , along with their statistical and systematic uncertainties, are shown in table II. Figure 4 shows the best fit ionization yield result as a function of the nuclear recoil energy, with a comparison with the standard Lindhard model. This result is not compatible with the Lindhard model for low energy values, as well as two other recent measurements that can be found in ref. [16] and ref. [17], which in turn are not compatible with each other. These inconsistencies may be due to temperature, electric field, or other in-situ effects. This situation suggests the need for more measurements with various experimental techniques, as well as the starting of a phenomenological campaign to solve this puzzle.

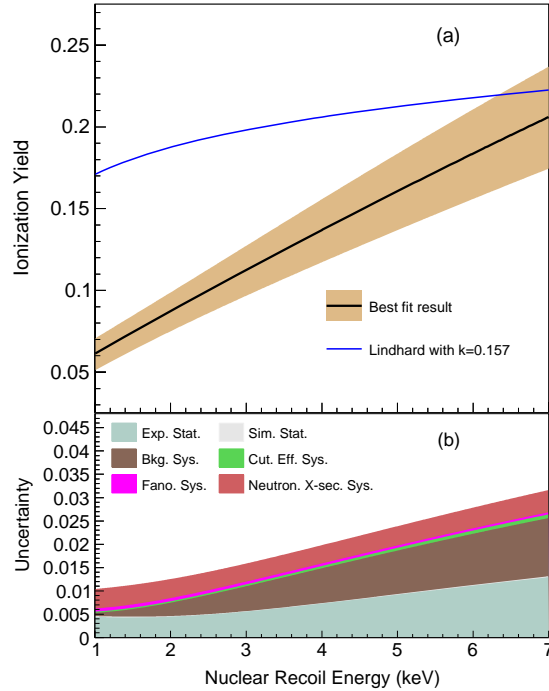


Fig. 4. – Top plot shows the ionization yield with the 1σ uncertainty from the best fit values as a function of the nuclear recoil energy in germanium. The blue line shows the standard Lindhard model with $k = 0.157$. Bottom plot shows the contribution of the statistical and systematic uncertainties. Taken from ref. [12].

REFERENCES

- [1] GREEN ANNE M., *Dark Matter in Astrophysics/Cosmology*, in *SciPost Phys. Lect. Notes* (SciPost) 2022, 37.
- [2] GOODMAN MARK W. and WITTEN EDWARD, *Phys. Rev. D*, **31** (1985) 3059.
- [3] KAPLAN D. E., LUTY M. A. and ZUREK K. M., *Phys. Rev. D*, **79** (2009) 115016.
- [4] ALEXANDER J. *et al.*, arXiv:1608.08632 (2016).
- [5] IRWIN K. D., NAM S. W., CABRERA B., CHUGG B. and YOUNG B. A., *Rev. Sci. Instrum.*, **66** (1995) 5322.
- [6] LUKE P. N., *J. Appl. Phys.*, **64** (1988) 6858.
- [7] NEGANOV B. S. and TROFIMOV V. N., *Otkryt. Izobret.*, **146** (1985) 215.
- [8] THE SUPERCDMS COLLABORATION, *Phys. Rev. D*, **95** (2017) 082002.
- [9] RAU W., GERBIER G., CAMUS P., DERING K., CAZES A., SCORZA S., ZHANG X. and DASTGHEIBI-FARD A., *J. Phys.: Conf. Ser.*, **1342** (2020) 012128.
- [10] THE SUPERCDMS COLLABORATION, arXiv:2203.08463 (2022).
- [11] YELLIN S., *Phys. Rev. D*, **66** (2002) 032005.
- [12] THE SUPERCDMS COLLABORATION, arXiv:2202.07043 (2022).
- [13] LINDHARD J. *et al.*, *Kgl. Danske Videnskab. Selskab. Mat. Fys. Medd.*, **33** (1963).
- [14] BARKER D. and MEI D.-M., *Astropart. Phys.*, **38** (2012) 1.
- [15] ALLISON J. *et al.*, *Nucl. Instrum. Methods Phys. Res. Sect. A*, **835** (2016) 186.
- [16] COLLAR J. I. *et al.*, *Phys. Rev. D*, **103** (2021) 122003.
- [17] BONHOMME A. *et al.*, arXiv:2202.03754 (2022).